ELSEVIER

Catalysis Today 44 (1998) 205–213

CATALYSIS TODAY

Properties of adsorbed oxygen on Au/SiO_2

Ki-Hyouk Choi[1], Byoung-Youl Coh, Ho-In Lee*

Division of Chemical Engineering, Seoul National University, Seoul 151-742, South Korea

Abstract

Oxygen adsorption on silica-supported gold catalyst from NO_2 and O_2 exposures were investigated by temperature-programmed desorption spectroscopy under a vacuum condition. NO_2 and O_2 exposures of the surface of the catalyst at room temperature gave adsorbed oxygen in atomic state. Adsorbed oxygen penetrated beneath the gold with lower activation energy for NO_2 exposure than for O_2 exposure. Adsorbed oxygen in oxidic state which was desorbed above 600 K altered the surface properties of gold and resulted in the decrease of activation energy for oxygen to penetrate beneath the gold surface.

Keywords: Oxygen adsorption; Au/SiO_2; Temperature-programmed desorption

1. Introduction

Gold was reported to enhance some reactions as a catalyst, although it was recognized to be very inert toward chemical reactions. Most of the reactions that were catalyzed by gold were related to oxygen species, for example, CO oxidation by O_2 [1–6], NO reduction by H_2 [7,8], oxygen exchange between CO and CO_2 [9], and NO_2 activation [10–13]. NO_2 activation by gold catalyst has attracted many researchers' attentions from the point of view of air pollutant reduction. Moreover, NO_2–gold catalytic system may give a new route for partial oxidation of hydrocarbon. In spite of practical interest for the above reaction system, there were only a few reports related to it in the chemical aspects. The nature of oxygen chemisorption on a gold surface was not explicitly established. Despite the disagreement on whether oxygen was chemisorbed on a gold surface, oxygen was believed to chemisorb on the supported gold surface [4,5,7,14,15]. In the case of unsupported gold surface, oxygen chemisorbed depending on the kind of oxygen-containing gas dosed. That is, dioxygen could not give the chemisorbed oxygen on the gold surface, but atomic oxygen could do that [16–30]. The high activation energy for chemisorption of oxygen may explain the above results. Bassi et al. [31] observed that the electronic properties of gold supported on Al_2O_3 and MgO were different from those of bulk phase gold, and they stated the strong interaction between gold and the support.

The understanding of the nature of chemisorbed species on a catalyst is very important to design and improve a catalytic system. In this paper, we present a study on the nature of oxygen chemisorbed on Au/SiO_2.

*Corresponding author. Tel.: 00 82 2 880 7072; fax: 00 82 2 888 1604; e-mail: hilee@plaza.snu.ac.kr

[1]Present address: HANWHA Group R&E Center, 6 Shinsung-dong, Yusung-ku, Taejon 305-345, South Korea.

0920-5861/98/$32.00
PII S0920-5861(98)00192-8

2. Experimental

The supported gold catalyst was prepared according to the following method:

- The support (Aerosil 200, Degussa, >99.8%) was impregnated into an appropriate amount of the aqueous solution of $HAuCl_4 \cdot 3H_2O$ (Aldrich, ACS reagent) for final catalyst to be 5 wt% gold loading.
- The slurry was dried at 363 K for 14 h in air.
- The dried sample was calcined at 1073 K for 4 h in air.
- The calcined sample was reduced at 723 K for 3 h in hydrogen flow.

The experiments were conducted in a vacuum chamber that was pumped by a triode sputter ion pump (Anelva) with pumping speed of 110 l/s. The base and working pressures of the chamber were 5×10^{-10} and 2×10^{-8} Torr, respectively. The total pressure of the chamber was monitored by a nude, Bayard-Alpert type ionization gauge (Varian), and the partial pressures of gases in the chamber were measured with a quadrupole mass spectrometer (Anelva, AGA-100). The sample was loaded on a stainless steel net (200 mesh) spot-welded on tantalum foil (0.025 mm thickness, Aldrich). The heating rate of the sample was fixed at 16.5 K/s through the experiments. The temperature of the sample was measured by a K-type thermocouple spot-welded on the center of the tantalum foil and controlled by a home-made temperature programmer [32]. An IBM-AT compatible micro-computer was used to measure the partial pressures of selected gases, total pressure of the chamber, and the temperature of the sample. NO_2 (Matheson, 99.5%) and O_2 (Aldrich, 99.9%) were purified by freeze-thaw method and acetone/dry-ice trap, respectively. The purities of gases were checked by mass spectra. Gas was dosed into the chamber through a variable leak valve (Varian). The sample was cleaned by several repetitions of heating–cooling cycle. The cleanliness of the sample was verified by reproducibility of temperature-programmed desorption (TPD) spectrum. Exposures reported here were expressed in the unit of Langmuir ($1\ L=1\times10^{-6}$ Torr s) taking into account the gauge sensitivity of each gas.

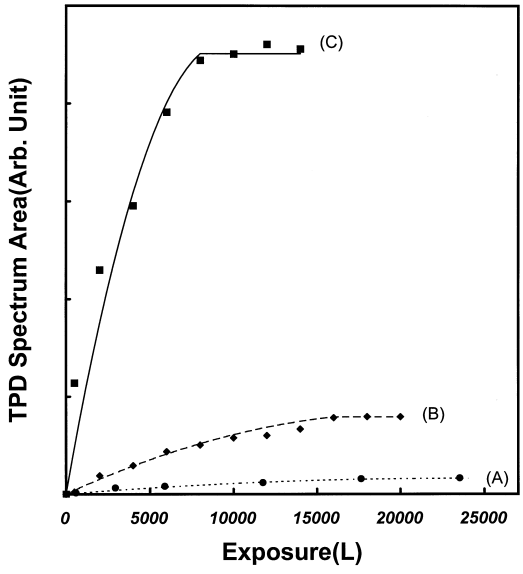

Fig. 1. (A) NO_2, (B) O_2, and (C) NO TPD spectrum areas after various NO_2 exposures at room temperature.

3. Results and discussion

NO_2, O_2 and NO TPD spectrum areas, which were not calibrated, after various NO_2 exposures of the sample at room temperature are shown in Fig. 1. The lack of stoichiometry in the desorbed O_2 is suggested to be mainly due to the difference in instrumental sensitivity of desorbing species, NO as a fragment of NO_2 during NO_2 desorption, and the penetration of surface oxygen into the bulk of the catalyst as discussed later. NO_2 exposure of the blank sample, which was consisted of tantalum foil, stainless steel net, and silica, gave very small amounts of desorption of gases compared with those in the case of the sample containing gold. Therefore, the adsorption and desorption of gases were regarded as to be occurred on gold, not silica. NO_2 is less stable than O_2. The bond energies of NO–O in NO_2 and O–O in O_2 are 73 and 119 kcal/mol, respectively, suggesting that NO_2 may be more easily decomposed on the surface than O_2. It was reported that NO_2 was not dissociatively adsorbed on the single [33] and polycrystalline [34] gold. However, there is no logical reason to apply the results on unsupported gold surface to supported gold surface, directly. Bassi et al. [31] proposed that gold supported on Al_2O_3 was in Au^{+1} state from their

EXAFS results suggesting that chemisorptive behavior on gold depends strongly on the catalyst type, that is, supported or unsupported. There is great discrepancy in chemisorption of NO on gold surface. Bartram and Koel [33] found that NO was not chemisorbed on unsupported gold surface. On the other hand, Lee and Schwank [8] observed the dissociative chemisorption of NO on silica-supported gold surface. As mentioned above, chemisorption of oxygen on gold surface gave similar results as the case of NO. There is no report about the interaction between NO_2 and supported gold catalyst. In our experiments, the amount of desorbed NO_2 was much smaller than that of NO after NO_2 exposures at room temperature (Fig. 1). The results suggest that most of NO_2 on the sample was decomposed into NO and O at the exposing temperature or during TPD. The disagreement with the results on unsupported gold surfaces [33,34] may be due to the different surface properties between the two types of gold.

Fig. 2 is O_2 TPD spectra after various NO_2 exposures at room temperature. The spectra show three different peaks at 340, 780, and 850 K. With the constant activation energy of desorption, TPD peak position is unchanged with exposure in the case of first order desorption, but changed in the case of second order desorption [35]. However, this is not the absolute criterion to determine the desorption order. We did not observe any change of peak positions in O_2 TPD spectra after NO_2 and O_2 exposures. Many researchers found that O_2 desorption followed a pseudo first order kinetics although oxygen is adsorbed in atomic state. To explore the state of oxygen species which was desorbed at 340 K, the plots of $\ln(R/C^n)$ with $1/T$ [36] were made to investigate desorption order, where R, n, C, and T are desorption rate, desorption order, coverage, and temperature, respectively (Fig. 3). The curve was linear only for $n=2$. The desorption activation energy calculated from the slope of the curve for $n=2$ was 18 kcal/mol, which agreed well with that calculated from Redhead method [36] by using pre-exponential factor of 10^{13} s^{-1} and heating rate of 16.5 K/s. The result suggests that desorption of oxygen which gave the peak at 340 K follows a second order kinetics due to recombinative desorption. The disagreement between the constancy of peak position and the result is hard to be explained. However, a deduction could be drawn out, that is, the peak position is too close to room temperature to be observed. The activation energy for O_2 desorption on unsupported gold surfaces

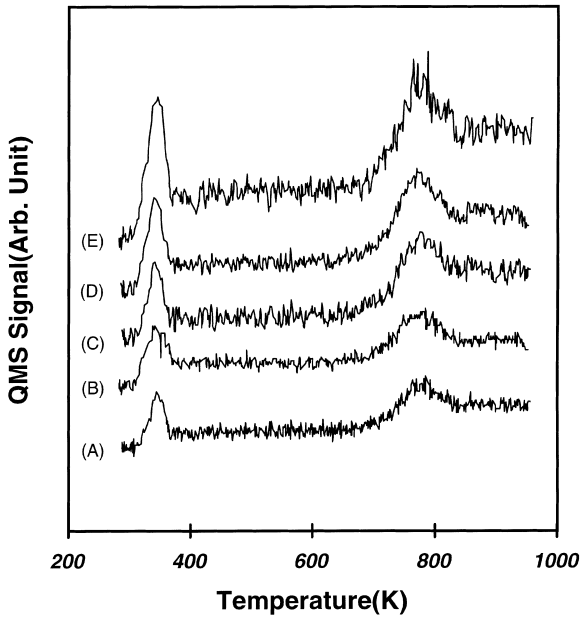

Fig. 2. O_2 TPD spectra after various NO_2 exposures at room temperature to (A) 2000 L, (B) 4000 L, (C) 8000 L, (D) 12 000 L, and (E) 16 000 L.

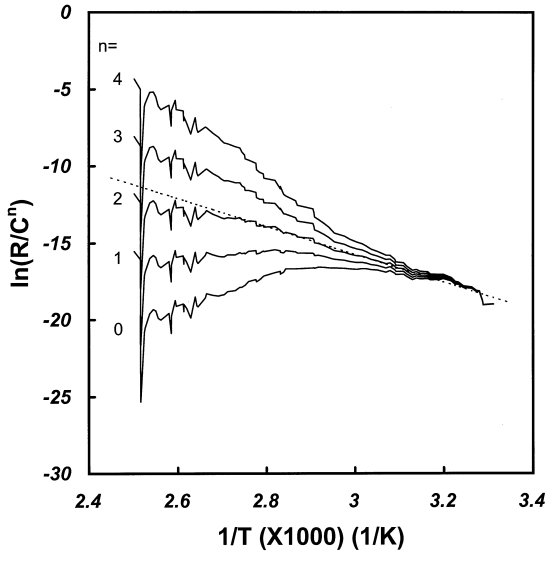

Fig. 3. Plots of $\ln(R/C^n)$ with $1/T$ for O_2 TPD spectrum after a 6000 L O_2 exposure at room temperature: R=desorption rate, C=coverage, n=desorption order, and T=temperature.

was reported to be 15–38 kcal/mol [16,23,25]. Taking into account the diversity of the activation energy for O_2 desorption, the energy obtained in this study agrees well with those reported on unsupported gold surfaces. Thus the adsorbed oxygen species which was desorbed at 340 K is considered to be oxygen adsorbed on the surface. Parker and Koel [23] estimated the activation energy for O_2 desorption on Au(1 1 1) with variation of oxygen coverage and found the increase of activation energy with coverage. They attributed the increase to the lateral interaction between adsorbed oxygens. However, the variation of peak temperature at 340 K was not observed in our study unlike their results. This seemed to be due to small particles of gold in our sample compared with the unsupported gold.

Although this study was focused on the qualitative properties of oxygen adsorbed on gold catalyst, we attempted to elucidate roughly the amount of oxygen adsorbed on our catalyst. The specific surface area measured by N_2 physical adsorption was 151 m^2/g and the surface composition (Au/Si) measured by XPS was 1.3 wt%. Surface area of gold supported on silica could be calculated to be about 3.2 m^2/g-catalyst with the assumption that gold was perfectly dispersed. Fukushima et al. [29] reported that surface area of gold on silica-supported gold catalyst (0.54–3.11 wt% Au) was 0.07–0.62 m^2/g-catalyst. From the above information, we could suggest the surface area of gold was some value in 0.2–3.2 m^2/g-catalyst. Fukushima et al. [29] proposed that adsorption stoichiometry of atomic oxygen on supported gold catalyst for saturated adsorption (Au/O) was 1–2 depending on exposure temperature. Therefore, the saturated amount of oxygen adsorbed on our catalyst could be calculated to be some value in 1.9×10^{-6}–6.1×10^{-5} mol/g-catalyst.

In spite of heating the sample up to 950 K during TPD, adsorbed oxygen seemed to remain on the sample after TPD because O_2 TPD line did not return down to the base line. Fig. 4 shows O_2 TPD spectra after 16 000 L NO_2 exposures at various temperatures. To remove the peak at 340 K for clarity, the sample was heated up to 600 K and cooled down to room temperature before getting each TPD spectrum. In Fig. 5, the area of O_2 TPD spectrum is plotted as a function of exposure temperature. The curve shows its maximum value at 600 K. A similar trend was observed when O_2 instead of NO_2 was dosed on the sample. Fig. 6 is the O_2 TPD spectra after 10 000 L O_2 exposures of the sample at various temperatures, and

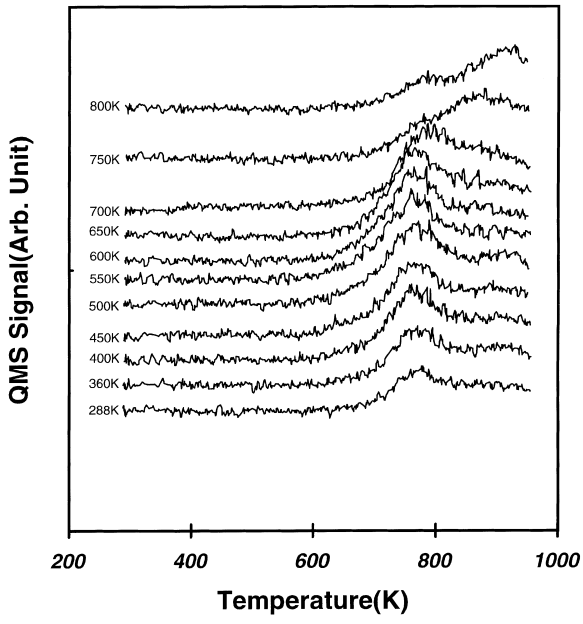

Fig. 4. O_2 TPD spectra after 16 000 L NO_2 exposures at various temperatures followed by heating upto 600 K and then cooling down to room temperature.

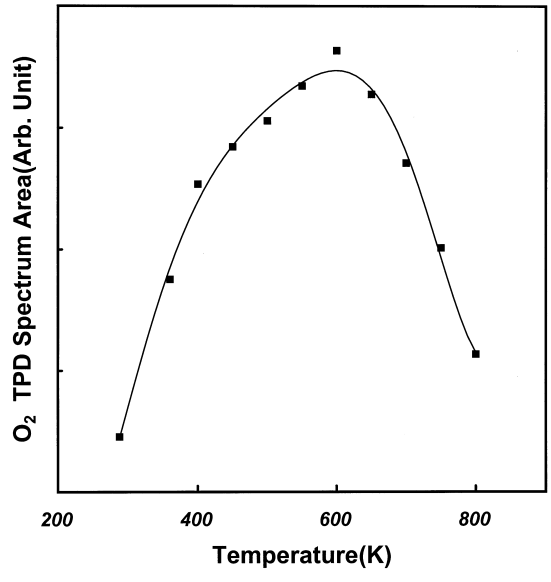

Fig. 5. O_2 TPD spectrum area vs. exposure temperature after 16 000 L NO_2 exposures at various temperatures followed by heating upto 600 K and then cooling down to room temperature.

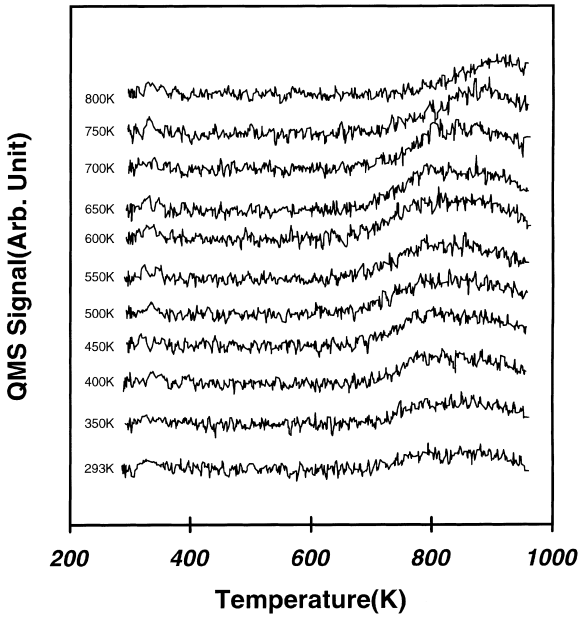

Fig. 6. O_2 TPD spectra after 10 000 L O_2 exposures at various temperatures followed by heating upto 600 K and then cooling down to room temperature.

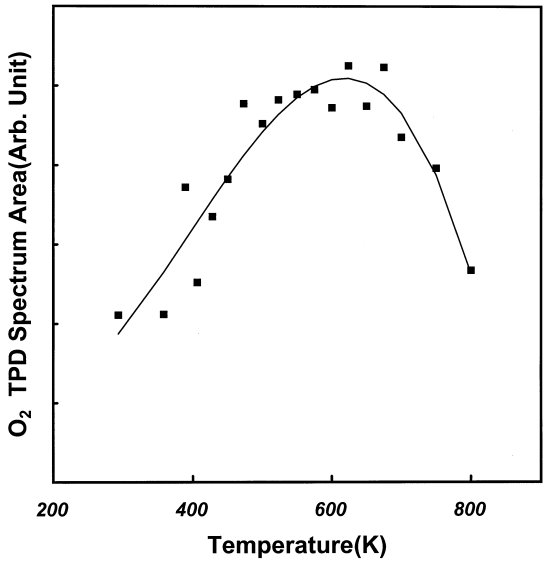

Fig. 7. O_2 TPD spectrum area vs. exposure temperature after 10 000 L O_2 exposures at various temperatures followed by heating upto 600 K and then cooling down to room temperature.

Fig. 7 is the corresponding curve to Fig. 5 for Fig. 6. When the sample was exposed to O_2 at room temperature only one desorption peak could be seen at 340 K, but a new peak appeared at 850 K by raising exposure temperature. The amount of O_2 desorbed was biggest at 650 K. In Figs. 5 and 7, the amount of oxygen desorbed increases with exposure temperature up to 600 K and then decreases. From the result, we conclude that the adsorption of oxygen which is desorbed above 600 K is an activated process. The decrease of O_2 TPD area above 600 K could be ascribed to the desorption of oxygen above 600 K. The activated process can be considered only to the oxygen species desorbed above 600 K. The same conclusion could be drawn for O_2 exposure from Fig. 7. The difference of maximum temperature by 50 K between Fig. 5 and Fig. 7 may be attributed to the differences in the shape and position of the oxygen peak desorbed above 600 K after NO_2 and O_2 exposures.

We attempted to find activation energies for adsorption of oxygen desorbed above 600 K from Arrhenius plots. Fig. 8 shows the Arrhenius plots for oxygen adsorption when O_2 (A) and NO_2 (B) were dosed on

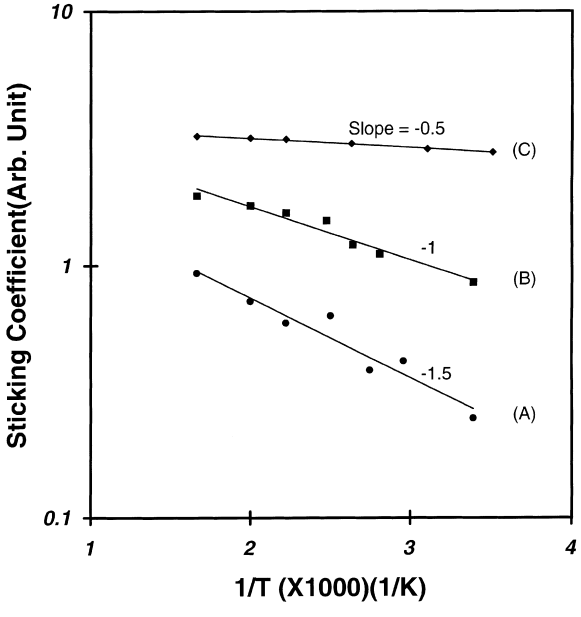

Fig. 8. Arrhenius plots for (A) O_2 and (B) NO_2 exposures of the clean sample, and (C) NO_2 exposures of the sample preadsorbed oxygen, which is prepared by a 5000 L NO_2 exposure of the clean sample at 600 K.

the sample. The adsorbed oxygen species considered in Fig. 8 was that desorbed above 600 K. Sticking

coefficient was obtained from the slope of the curve of exposure vs. O_2 TPD area [37]. Curve (C) was obtained when NO_2 was dosed on the oxygen-covered sample, which was prepared by a 5000 L NO_2 predosing on the sample at 600 K. The slopes of the curves in Fig. 8 are 1.5 for curve (A) and 0.5 for curve (C) when the slope of curve (B) is referenced to −1. It is the most interesting feature in the Arrhenius plots that the slope is smaller for NO_2 exposure than for O_2 exposure. This suggests that NO_2 is more readily adsorbed to produce the oxygen species desorbed above 600 K than O_2. This difference in activation energy for production of the adsorbed oxygen species which is desorbed above 600 K could be attributed to smaller bond energy of NO–O than that of O–O, whose ratio is about 1.6. It is simply deduced from comparing this ratio with that of activation energies that the key step for production of the adsorbed oxygen species desorbed above 600 K is the bond dissociation of NO–O and O–O. However, we must consider the presence of co-adsorbed NO when NO_2 is dosed on the sample because co-adsorbed NO may alter the surface condition and adsorption state of oxygen.

To explore the effect of co-adsorbed NO on oxygen chemisorption in detail, we tried a subsequent exposure experiment. The result is in Fig. 9, in which curve (A) is O_2 TPD spectrum after a 2000 L NO_2 exposure at 750 K followed by a 5000 L NO exposure at room temperature and curve (B) is the arithmetically added spectrum of two O_2 TPD spectra after a 2000 L NO_2 exposure at 750 K and after a 5000 L NO exposure at room temperature, separately. The NO_2 exposure temperature was selected to 750 K to suppress the desorption peak of 750 K, which did not come out after O_2 exposure. The most distinct feature in two spectra is intensification of desorption rate at about 750 K in spectrum (A). This suggests that desorption peak at 750 K, which appears only when NO_2 is dosed, is related to the presence of co-adsorbed NO. NO is regarded as an acidic ligand in organometallic complex, which means the ability of NO to accept electron density from metal [38]. So, adsorbed NO on gold surface could be supposed to withdraw electron density from gold and make gold more positive. The conclusive evidence could be found in Fig. 8(C), which is the result on the oxygen-precovered sample. Like NO, oxygen may alter the chemisorption properties of the gold because of its high electronegativity. The slope of the curve which correlates with the activation energy for the production of adsorbed oxygen species was sharply decreased to 0.5 agreeing with the intensification of desorption rate at about 750 K in spectrum (A) of Fig. 9. From the result, it is very clear that the activation energy for production of adsorbed oxygen species desorbed above 600 K is dominated by the surface condition of gold, which is sensitive to the presence of co-adsorbed NO or oxygen.

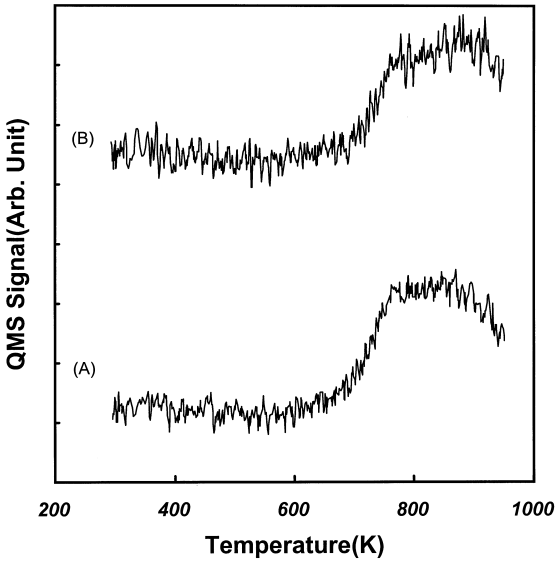

Fig. 9. (A) O_2 TPD spectrum after a 2000 L NO_2 exposure at 750 K followed by a 5000 L NO exposure at room temperature and heating upto 600 K and then cooling down to room temperature. (B) Arithmetically added O_2 TPD spectrum of those after a 2000 L NO_2 exposure of the sample at 750 K and after a 5000 L NO exposure at room temperature. Both exposures were followed by heating upto 600 K and then cooling down to room temperature.

Gold was reported to be changed to oxide state when it was treated under severe oxidative condition. Chesters and Somorjai [17] observed that the oxide layer formed on Au(1 1 1) surface was very stable up to 1173 K compared with bulk oxide (Au_2O_3) which was known to decompose near 413 K. They observed that adsorbed oxygen could be removed from the gold surface by heating at 1073 K during 12 h under vacuum. They attributed the abnormal stability of the oxide layer to the unique property of the surface. This stable oxide state was also reported by Schrader [18], who reported the activation energy of 6 kcal/mol

to form this state from O_2 on Au(1 1 1). Furthermore, in his report, migration of oxygen from active site on which oxygen was dissociated to less active site and diffusion of oxygen into gold lattice were presented. He also observed abnormal stability of adsorbed oxygen. It was found by Canning et al. [25] that O(1s) electron binding energy of oxygen in the surface oxide formed on unsupported gold was closer to that of adsorbed oxygen rather than that of oxygen in bulk oxide (Au_2O_3). Their suggestion was consistent with the TPD spectrum in which only one peak was shown and O/Au ratio of 2, which implied that only a shallow oxide layer was formed in gold.

In our study, two kinds of oxygen present in gold could be discriminated clearly in TPD spectrum. Being judged by those peak temperatures, there might be a great difference in adsorption enthalpy. It is worthy to notify that there was somewhat desorption process between two desorption regions, as mentioned above. The desorption in that region implies that transition of oxygen from weakly bound state to strongly bound one or vice versa. Thus the activation energy obtained from Fig. 8 could be attributed to the activation energy required for oxygen to change from the adsorbed state which was desorbed at 340 K to that which was desorbed above 600 K. The reverse transition from strongly bound state to weakly bound one can be seen in Fig. 10, which is a set of O_2 TPD spectra after 10 000 L NO_2 exposures of the sample at room temperature followed by heating up to various temperatures and cooling down to room temperature. Above annealing temperature of 700 K, the peak at 340 K was re-emerged. It is very interesting that the desorption peak of 340 K is re-emerged when annealing temperature is above 700 K. This indicates again that oxygen can move from one state to the other state if thermal energy is supplied to overcome the barrier. This supports the previous discussion about lower activation energy for NO_2 exposure in Fig. 8.

Now, the remained question is what kind of adsorbed oxygen is responsible for the oxygen desorption above 600 K. As mentioned above, the oxygen species desorbed at 340 K is atomic species, so we can guess that surface heterogeneity may give rise to such a great difference in desorption temperature. However, the difference is too great to be ascribed simply to surface heterogeneity. The presence of oxidic oxygen in gold was known for several decades. Thus the

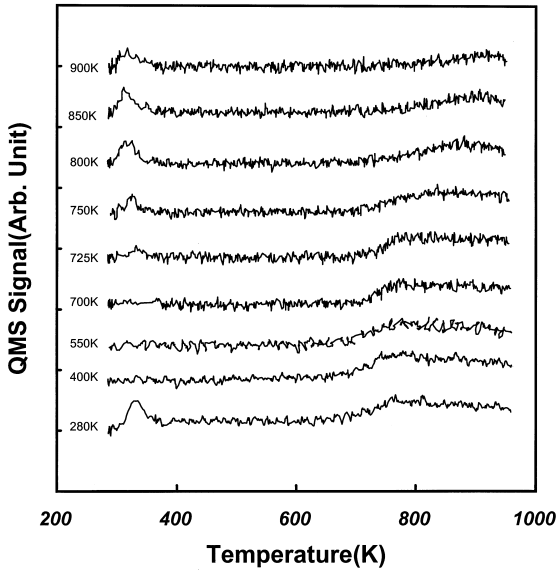

Fig. 10. O_2 TPD spectra after 10 000 L NO_2 exposures at room temperature followed by heating upto various temperatures and then cooling down to room temperature.

oxygen species desorbed above 600 K was concluded to be oxygen in oxide phase since it shows a very high desorption temperature and has high activation energy barrier. Another evidence could be found from the O_2 TPD spectrum after NO_2 exposure, in which there is some desorption between the two desorption regions. The similar results could be seen in the literature concerned with oxygen adsorption on Ag powder [39], in which a new peak appeared at 850 K when O_2 was exposed on Ag powder at 453 K. The O_2 desorption peak at such a high temperature was reported to appear only on rough surface which has many kinks and steps. The authors of the literature proposed the origin of the desorption peak at 850 K to be subsurface oxygen. This indicates that more subsurface oxygen can be produced on rough surface than smooth one. The lower activation energy for adsorption in this study might be ascribed to large density of steps and kinks. For Pd, the density of surface imperfections was reported to influence the readiness for oxygen to penetrate beneath the surface [40]. So, oxygen may migrate into the subsurface more easily in our supported sample than in unsupported one. The decrease of activation energy for adsorption in the oxygen precovered gold can be explained by the

shrinkage of gold atom radius, which makes oxygen diffuse more easily, when gold is oxidized. Formal charge of oxidic gold was indicated as +1 by Canning et al. [25]. As their experiments, gold atom in our oxidized sample could be regarded as to have +1 charge. Thus, gold atom in oxidized sample has shorter atomic radius than that in non-oxidized sample. Therefore, oxygen in oxidic phase may alter the electronic and geometric properties of gold, consequently chemisorption properties of gold.

Some investigators insisted that impurities in gold were responsible for oxygen adsorption and that gold without impurity did not adsorb oxygen [19,21,22,25]. The impurities that can affect the adsorption properties were reported to be calcium and silicon, which formed stable oxides by reaction with oxygen. We could not exclude definitely the possibility that oxygen was bound to the impurities which might be in the sample. However, the reagents used for preparation of the sample were very highly pure and calcination temperature was so high that all the impurities were converted into the oxides which were very stable [41]. Additionally, there was no characteristic peak of calcium on XPS data of the sample. Anyway, although the contribution from impurity could not be excluded, the peculiar properties of supported gold sample could be ascribed to strong interactions between support and gold or to surface heterogeneity of gold, both of which are absent in the case of unsupported gold surface.

The chemisorptive behavior of gold is similar to that of silver in many aspects. For example, there are lateral interactions between adsorbed oxygen atoms on both surfaces and activation barrier for oxygen to diffuse into the bulk [42]. For silver, subsurface oxygen was known to play an important role in ethylene epoxidation by increase of the binding energy oxygen–ethylene bond and decrease of adsorption energy of oxygen on the surface [43]. In analogous context, oxygen in oxidic phase of gold can be considered as an important reagent in partial oxidation of hydrocarbon.

4. Conclusion

Oxygen was adsorbed on silica-supported gold surface as an atomic state. Adsorbed oxygen on gold surface could be discriminated into two kinds, which were chemisorbed one on gold surface and oxidic one beneath the surface. Transition between two states required an activation energy, which was estimated to be 1.5 times larger for O_2 exposure than for NO_2 exposure. The activation energy for production of oxidic oxygen depended strongly on the surface condition which was sensitive to co-adsorbed species. On 'oxidized' surface, oxygen more easily penetrated beneath the surface.

Acknowledgements

We would like to thank Prof. Jae Sung Lee at POSTECH, Korea for the donation of NO_2 gas. KHC acknowledges the financial support from HANWHA group in the form of scholarship.

References

[1] S.D. Gardner, G.B. Hoflund, B.T. Upchurch, D.R. Schryer, E.J. Klei, J. Schryer, J. Catal. 129 (1991) 114.
[2] M. Haruta, T. Kobayashi, H. Sano, N. Yamada, Chem. Lett. (1987) 405.
[3] M. Haruta, N. Yamada, T. Kobayashi, S. Iijima, J. Catal. 115 (1989) 301.
[4] S. Lin, M.A. Vannice, Catal. Lett. 10 (1991) 47.
[5] S. Lin, M. Bollinger, M.A. Vannice, Catal. Lett. 17 (1991) 245.
[6] N.W. Cant, P.W. Fredrickson, J. Catal. 37 (1975) 531.
[7] S. Galvagno, G. Parravano, J. Catal. 55 (1978) 178.
[8] J.Y. Lee, J. Schwank, J. Catal. 102 (1986) 207.
[9] D.Y. Cha, G. Parravano, J. Catal. 18 (1970) 200.
[10] N. Pourreza, S.A. Montzka, R.M. Barkley, R.E. Sievers, R.S. Hutte, J. Chromatogr. 399 (1987) 165.
[11] S.A. Nyarady, R.M. Barkley, R.E. Sievers, Anal. Chem. 57 (1985) 2074.
[12] M.J. Bollinger, R.E. Sievers, D.W. Fahey, F.C. Fehsenfeld, Anal. Chem. 55 (1983) 1980.
[13] S.A. Nyarady, R.E. Sievers, J. Am. Chem. Soc. 107 (1985) 3726.
[14] J. Schwank, S. Galvagno, G. Parravano, J. Catal. 63 (1980) 415.
[15] A.G. Shastri, A.K. Datye, J. Schwank, J. Catal. 26 (1984) 265.
[16] A.G. Sault, R.J. Madix, C.T. Campbell, Surf. Sci. 169 (1986) 347.
[17] M.A. Chesters, G.A. Somorjai, Surf. Sci. 52 (1975) 21.
[18] M.E. Schrader, J. Colloid Interface Sci. 59 (1977) 456.
[19] J.J. Pireaux, M. Chtaib, J.P. Pelrue, P.A. Thiry, M. Liehr, R. Caudano, Surf. Sci. 141 (1984) 221.
[20] N.N. Dobrovolskii, V.E. Ostrovskii, A.M. Rubashov, M.I. Temkin, Chem. Abstr. 70 (1969) 99938.

[21] P. Legare, L. Hilaire, M. Sotto, G. Maire, Surf. Sci. 91 (1980) 75.
[22] D.D. Eley, P.B. Moore, Surf. Sci. 76 (1978) L599.
[23] D.H. Parker, B.E. Koel, J. Vac. Sci. Technol. A 8 (1990) 2585.
[24] D.A. Outka, R.J. Madix, Surf. Sci. 179 (1987) 351.
[25] N.D.S. Canning, D. Outka, R.J. Madix, Surf. Sci. 141 (1984) 240.
[26] P.C. Richardson, D.R. Rossington, J. Catal. 20 (1971) 420.
[27] W.R. MacDonald, K.E. Hayes, J. Catal. 18 (1970) 115.
[28] N. Endow, B.J. Wood, H. Wise, J. Catal. 15 (1969) 316.
[29] T. Fukushima, S. Galvagno, G. Parravano, J. Catal. 57 (1979) 177.
[30] N.P. Kulkova, L.P. Leveshenko, Kinet. Catal. 6 (1965) 688.
[31] I.W. Bassi, F.W. Lytle, G. Galvagno, J. Catal. 42 (1976) 139.
[32] K.-H. Choi, H.-I. Lee, Inst. Sci. Technol. 22 (1994) 73.
[33] M.E. Bartram, B.E. Koel, Surf. Sci. 213 (1989) 37.
[34] D.T. Wickham, B.A. Banse, B.E. Koel, Catal. Lett. 6 (1990) 63.
[35] P.A. Redhead, Vacuum 12 (1962) 203.
[36] D.H. Parker, M.E. Jones, B.E. Koel, Surf. Sci. 233 (1990) 65.
[37] H.-I. Lee, Ph.D. Thesis, The University of Texas at Austin, 1979, p. 66.
[38] F.A. Cotton, G. Wilkinson, Advanced Inorganic Chemistry, Wiley, New York, 1988, p. 305.
[39] M. Bowker, P. Pudney, G. Roberts, J. Chem. Soc., Faraday Trans. 1 85 (1989) 2635.
[40] D.L. Weisman, M.L. Shek, W.E. Spicer, Surf. Sci. 92 (1980) L59.
[41] A. Cros, F. Salvan, M. Commandre, J. Derrien, Surf. Sci. 103 (1981) L109.
[42] R.A. van Santen, H.P.C.E. Kuippers, Adv. Catal. 35 (1987) 265.
[43] P.J. van den Hoek, E.J. Baerends, R.A. van Santen, J. Phys. Chem. 93 (1989) 6469.